Contents lists available at UGC-CARE

International Journal of Pharmaceutical Sciences and Drug Research

[ISSN: 0975-248X; CODEN (USA): IJPSPP]

journal home page : http://ijpsdronline.com/index.php/journal

Research Article

In-silico Evaluation of Phytochemicals from *Calotropis gigantea* (L.) Dryand. for Multi-Target Inhibition of Cobra Venom Proteins

Aswathy Chandran, Sreekumar S*, Keerthi Sugathan J, Biju CK

Biotechnology & Bioinformatics Division, Saraswathy Thangavelu Extension Centre, KSCSTE-Jawaharlal Nehru Tropical Botanic Garden & Research Institute, A Research Centre of Kerala University, Puthenthope, Thiruvananthapuram, Kerala, India.

ARTICLE INFO

Article history:

Received: 18 December, 2024

Revised: 09 February, 2025

Accepted: 12 February, 2025

Published: 30 March, 2025

Keywords:

Cobra venom, *Calotropis gigantea,* Molecular docking, MD simulations, Multi-targets, Phospholipase A_2, Phytochemicals, ADMET.

DOI:

10.25004/IJPSDR.2025.170203

ABSTRACT

Snake envenomation leads to about 125,000 deaths yearly worldwide, with India accounting for almost 50,000 of these fatalities. Even as antivenoms remain the primary treatment, they have limitations, prompting the exploration of phytochemicals from *Calotropis gigantea* as potential multi-target therapies against cobra venom toxins. About 14 venom proteins, namely phospholipase A_2 (PLA_2), cobrotoxin, L-amino acid oxidase, acetylcholinesterase, cobramin A, cobramin B, cytotoxin 3, long neurotoxins 1 to 5, serine protease and proteolase were the selected targets. The 3D structures of those venom proteins were downloaded from the protein data bank and SWISS-MODEL. A complete of 164 phytochemicals from *C. gigantea* were docked using AutoDock Vina and PyRx 8.0 to assess their binding capability. Compounds with binding energies ≤ -6 kcal/mol have been selected as hits based on their multi-target activity. Subsequently, absorption, distribution, metabolism, excretion, and toxicity (ADMET) properties and molecular interactions of these molecules were analyzed, with choice standards specializing in binding affinity and pharmacokinetics. Molecular dynamics simulations over 100 ns, completed the usage of GROMACS 2018.1, identified β-amyrin and lupeol as effective inhibitors of PLA_2, acetylcholinesterase, and cobrotoxin. Lupeol exhibited greater constancy throughout simulations, at the same time as β-amyrin more suitable enzyme structure stabilization. Both compounds demonstrated good pharmacokinetics, though issues such as low solubility and potential cardiac dangers warrant further research.

Introduction

Snakebite is an intense global health hazard, especially in tropical areas, causing ~ 125,000 deaths every year, with ~50,000 deaths going on in India.[1] Because of the excessive mortality rate, the World Health Organization (WHO) covered snakebites under the category of neglected tropical disease.[2]

Snake venom is an incredibly tricky biochemical aggregate commonly composed of enzymes and non-enzymatic proteins. It constitutes about 90% of proteins.[1] It also carries small quantities of carbohydrates, lipids, and metal ions. The enzyme components show various activities, such as metalloproteinase, serine proteinase, phospholipase A_2 (PLA_2), acetylcholinesterase (AChE), L-amino acid oxidase (LAAO), and hyaluronidase. Non-enzyme products include natriuretic peptides, 3-finger toxins, C-type lectins, protease inhibitors, and bradykinin-enhancing peptides. The current treatment for snakebites is anti-venom therapy, however, its barriers consist of the dangers of hypersensitive reactions, high costs, and trouble in identifying the snake species.[3] Because venom has many constituents that cause illness and death, a "one drug, one target" approach will not work. Phytochemicals that may block a couple of targets simultaneously offer promise.[1]

Research highlights the capacity of plant-derived molecules as drugs, noting their structural significance, safety, diverse activity, stability, and novelty. Many

***Corresponding Author:** Dr. Sreekumar S

Address: Biotechnology & Bioinformatics Division, Saraswathy Thangavelu Extension Centre, KSCSTE-Jawaharlal Nehru Tropical Botanic Garden & Research Institute, A Research Centre of Kerala University, Puthenthope, Thiruvananthapuram, Kerala, India.

Email ✉**:** drsreekumar@rediffmail.com

Tel.: +91-9446480968

Relevant conflicts of interest/financial disclosures: The authors declare that the research was conducted in the absence of any commercial or financial relationships that could be construed as a potential conflict of interest.

snakebite victims still are seeking for herbal healers. Evaluating the effectiveness and safety of these practices could cause the development of new remedies for snake envenomation.

Calotropis gigantea (L.) Dryand., (family Apocynaceae), is a common wasteland plant native to India, thriving at altitudes up to 900 m. Different parts of this plant such as roots, bark, leaves, flowers, and latex, are widely used in conventional drug treatments consisting of Ayurveda, Unani, and Siddha. The latex, released when tissues are injured can be used to treat illnesses like fever, rheumatism, indigestion, respiratory tract infections, skin diseases and belly ulcers. Despite its high medicinal value, its potential as an antivenom remains unexplored.

The Indian cobra (*Naja naja*), a venomous snake causing a high rate of mortality, provides venom that spreads speedily due to the motion of hyaluronidase, leading to a high fatality rate. This research investigates the capability of phytochemicals from *C. gigantea* to neutralize cobra venom *via* inhibiting its toxic proteins using *in-silico* methods.

Materials And Methods

Target Preparation – Venom Toxic Proteins

Fourteen cobra venom proteins have been selected for analysis as described in previous publications.[1] Three-dimensional (3D) structures of phospholipase A_2 (PDB ID: 1A3D) and cobrotoxin (PDB ID: 1COD) were received from the PDB. 3D models had been prepared the use of predictive models for L-amino acid oxidase and acetylcholinesterase.[3] The remaining proteins, include cobramin A (SwissProt ID: P01447), cobramin B (SwissProt ID: P01440), cytotoxin 3 (SwissProt ID: P24780), long neurotoxins 1 to 5 (SwissProt IDs: P25668, P25669, P25671, P25672, P25673), and proteolase (SwissProt ID: Q9PVK7) are all from the SWISSMODEL repository.[1] The tools Q-site Finder and Pocket Finder have been used for detecting active sites of all proteins.

Ligand Preparation

A comprehensive evaluation of literature and publicly available chemical databases revealed around 164 phytochemicals from *C. gigantea*. 3D models of those compounds were downloaded from PubChem in canonical SMILES format after which modeled in CORINA software. Preparation of docking targets and ligands followed the procedure developed by Nisha *et al.* [3]

Molecular Docking

The docking tool AutoDock Vina integrated with PyRx 8.0 (https://pyrx.sourceforge.io) was used to assess interactions between the target proteins and the 164 ligands.[4] The docking technique followed the method outlined by Shefin *et al.*[5] Docking complexes (target and ligand) with binding free energy ≤ -6 kcal/mol were considered as hits. Compounds that inhibited more than three targets have been further screened to determine ADMET properties and protein-ligand interactions to identify the most promising candidates.

Post-Docking Analysis

Discovery Studio Visualizer analyzes protein ligands with a focus on optimizing hydrogen bond interactions. Physicochemical and ADMET properties were evaluated using the pkCSM tool and results were interpreted with the principles of Douglas *et al.*[6] The top-ranked five hits were subjected to pharmacokinetic evaluation using the SwissADME online tool.[7] The analysis included molecular descriptors such as molecular weight, number of hydrogen bond donors and acceptors, logP value, compliance with Lipinski's rule of five, and toxicity predictions. The molsoft prediction tool was used to evaluate the drug-likeness properties of the promising hits.

Molecular Dynamic Simulation

GROMACS 2018.1 software was used for molecular dynamics (MD) simulations. Selected protein-ligand complexes have been simulated using CHARMM force fields in a dodecahedral box with periodic boundary conditions. The system changed into dissolved with spc/216 standard water and Na+ and Cl^- ions were introduced to neutralize the protein. Energy reduction was performed up to 50,000 steps using the maximum descent rate and stopped when the maximum energy dropped under 10.0 kJ/mol. The first stage was performed at a constant particle number, volume, and temperature (NVT) of 300 K for 100 ps using the leapfrog integration algorithm and the V-rescaling thermostat. In the second stage, a constant particle number, pressure, and temperature (NPT) check was achieved using the Berendsen barostat, keeping the pressure at 1 bar for 100 ps. After equilibrium was reached, a couple of MD simulations were performed for 100 ns, and the trajectory data were recorded every 2 fs. MD trajectory evaluation consists of the calculation of the root mean square deviation (RMSD), root mean square fluctuation (RMSF), a radius of gyration (Rg), and H-bond interactions between the protein-ligand complex and the solvent.

Results And Discussion

Snake venoms are divided into four groups in line with their therapeutic outcomes: neurotoxicity, hemotoxicity, cytotoxicity and myotoxicity. Among their proteins, phospholipase A_2 (PLA_2) plays a vital function and shows various effects. PLA_2 is a key enzyme within the venom that causes extreme cell harm and inflammation with the aid of hydrolyzing phospholipids in cell membranes. This impact ends in the cytotoxic, neurotoxic, and myotoxic consequences of the venom, which cause the intense signs and symptoms visible in snakebite sufferers.[8,9]

Cobrotoxin, a neurotoxic peptide found in cobra venom, disrupts neuromuscular transmission with the aid of

binding to acetylcholine receptors, causing paralysis and respiratory failure.[10,11] Another component of the venom, L-amino acid oxidase (LAAO), produces keto acids, ammonia and hydrogen peroxide by catalyzing the oxidative deamination of L-amino acids with the help of flavin adenine dinucleotide (FAD) as a cofactor. Hydrogen peroxide produced in the course of this time can cause oxidative stress and cell damage.[12–14] Interestingly, LAAO has been investigated for its application in cancer treatment.[15,16]

Acetylcholinesterase (AChE) plays an important role in neurotransmission *via* breaking down acetylcholine into acetate and choline, Its inhibition can lead to excessive disruption of neurotransmission leading to muscle twitching and convulsions, which are the consequences of neurotoxins.[17-20] The usage of AChE inhibitors within the remedy of myasthenia gravis and Alzheimer's disease highlights their importance in the study of neurotransmission and cholinergic control.[21,22]

Cobramin A, a neurotoxic protein in cobra venom, disrupts neuromuscular transmission and may lead to paralysis.[23] Another neurotoxic agent is cobramin B, which impacts neuromuscular function and increases the overall toxicity of the venom.[24] Cytotoxin 3 is a cytotoxic protein that disrupts cellular membranes and motive cell lysis and has potential applications in cellular biology and most cancer research.[25]

Cobra venom long neurotoxins 1–5 possess an awesome three-fingered fold shape that permits it to engage with nicotinic acetylcholine receptors on the neuromuscular junction, in the long run, inflicting paralysis. Mutations in its loop may additionally have receptor binding and neurotoxic consequences and might provide insight into receptor interactions and healing capability.[23-25]

Cobra venom serine protease, part of the three-finger toxin family, is a potent cytotoxin that breaks the shape of cellular membranes, causing cell lysis and tissue damage, specifically within the coronary heart muscle.[26] Its compact structure increases membrane permeability, leading to negative outcomes along with hemolysis and cardiotoxicity.[8] Extensive research has been performed to elucidate its mechanism of action and to analyze its potential therapeutic uses.[27]

Cobra venom proteolases, or metalloproteinases, are zinc-containing enzymes that degrade proteins by hydrolyzing peptide bonds. They break proteins in the extracellular matrix, impair blood clotting, purpose infection, and exacerbate pain and tissue harm.[28,29]

In-silico research, is pivotal in drug discovery, enabling efficient screening, correct prediction of drug interactions, and decrease the need for laboratory testing. Notable examples consist of the development of sitagliptin for the remedy of type 2 diabetes and nivolumab for the remedy of cancer, both of which have been optimized using computational strategies.[30-33] In this context, we performed an *in-silico* analysis of a total of 164 phytochemicals from *C. gigantea* against the above-noted 14 targets in cobra venom using the widely used open-source molecular docking tool, AutoDock Vina.[34,35] The docked outcomes were used to visualize the ligand binding poses, analyze the expected binding relationships, examine the interactions with the target protein, and compare the results as shown by Trott and Olson.[1,4,36] However, the free energy of binding is critical for the preliminary selection of lead compounds as it presents many indicators about the stability and strength of the ligand-target interactions, which in turn influences the performance and efficacy of the lead compounds.[4,31,37] Strong binding affinity is usually associated with ΔG_bind values of ≤ -7.0 kcal/mol, while values between -5 and -7 kcal/mol imply slight binding and values above -5 kcal/mol suggest susceptible interaction strength. A threshold value of -6 kcal/mol is regularly used to identify potential hits.[38,39] In this have a look at, molecules with a ΔG_bind of ≤ -6 kcal/mol have been taken into consideration as hits or promising candidates.

The docking analysis (Table 1) indicated that 40 out of 164 phytochemicals didn't gain binding energies of ≤ -6 kcal/mol with any target. From the last 124 phytochemicals, the hits for each target were distributed as follows: acetylcholinesterase (80), L-amino acid oxidase (70), cobratoxin (62), serine protease (30), proteolase (7), long neurotoxins (1–5 hits per target), phospholipase A2 (5), cytotoxin (3), cobramin B (3), and cobramin A (2). Of the 80 phytochemicals interacting with acetylcholinesterase, 47 had ΔG_bind value ≤ -7.0 kcal/mol, while the best binding energy of proceroside was found to be -9.6 kcal/mol. Further, 22 out of 70 compounds targeting L-amino acid oxidase had ΔG_bind of ≤ -7.0 kcal/mol and rutin had the least binding energy of -11.5 kcal/mol. In the case of cobratoxin, 27 phytochemicals were found to have binding energy of ≤ -7.0 kcal/mol, and β-amyrin showed the least binding energy (-8.9 kcal/mol).

Serine protease showed ΔG_bind of ≤ -7.0 kcal/mol in three out of 30 identified hits, among which sapogenins had the lowest binding energy of -7.4 kcal/mol. For proteolase, β-amyrin and lupeol showed the lowest ΔG_bind value of -9.5 kcal/mol, while five out of seven candidates had a ΔG_bind value of ≤ -7.0 kcal/mol. All compounds targeting long neurotoxin 1-5 showed a ΔG_bind of ≤ -7.0 kcal/mol, while β-amyrin showed a minimum binding energy ranging from -7.4 to -7.6 kcal/mol. Similarly, long neurotoxin 2 of four compounds reached a ΔG_bind of ≤ -7.0 kcal/mol. Phospholipase A_2 had three compounds with ΔG_bind value of ≤ -7.0 kcal/mol, while rutin had the lowest binding energy, -7.6 kcal/mol, followed by β-amyrin, -7.4 kcal/mol. The lowest ΔG_bind value was recorded as -6.1 kcal/mol for cytotoxin 3, lupeol and β-amyrin. For cobramin B, β-amyrin showed the least binding energy (-6.7 kcal/mol), while for cobramin A, both β-amyrin and lupeol showed a binding energy -6.1 kcal/mol.

Table 1: List of phytochemicals selected as ligand from *C. gigantea* and binding energy between each of the phytochemicals and 14 selected cobra venom proteins

S. No.	*Phytochemicals*	*Targets*												
		PLA_2	*COT*	*LN 1*	*LN 2*	*LN 3*	*LN 4*	*LN 5*	*CA*	*CB*	*CYT 3*	*PL*	*SP*	*L-AAO*	*AchE*
1	Gigantursenyl acetate A (100998320)	232	**-7.4**		1.6	179.6	105.4	-3.3	169.8	97.8	3.9	7	**-6.7**	35.2	**-8.7**
2	Proceroside	385.2	-6.9		101.4	329.6	191.3	3.1	301.8	212.7	16		-6	61.3	-9.6
3	Quercetin 3-rutinoside-7-glucoside	142.4	-7		12.2	92.1	42.3	-3.7	111.2	78.7	2.7	5.6	-7	20.5	-9.2
4	Methyl dihydrojasmonate	-1.5	-4.9	29.1	-3.5	-3.4	-3.7	-3.8	-1.9	-2.1	-3.2	-4.1	-4	-6.8	-5
5	2,4-Bis(1-phenylethyl)phenol	16.8	-7.4	55	-4.5	2.7	-3.7	-4.2	13.5	-1	-4.2	-6	-6.6	-6.7	-8
6	1,4-Diaminobutane	-3.1	-3.2	-0.4	-2.2	-2.4	-2.9	-2.8	-2.3	-1.8	-2	-2.2	-2.5	-3.5	-3.1
7	Arachidic acid	7.1	-5.7	31.7	-3.8	-2.1	-2.8	-2.8	3.3	-1.3	-3.2	-3.5	-3.5	-6.7	-4.7
8	Triacontanoic acid	30.4	-6	57.1	-2.9	7.5	-1.3	-2.9	24.8	1	-3.2	-2.8	-3	-4.3	-4.6
9	1,3,4,5-tetrahydroxycyclohexanecar-boxylic acid	1.9	-4.4	24.8	-3.4	-4.1	-3.7	-4.1	-3.3	-3	-3.7	-3.9	-4	-5.8	-4.8
10	Dictyoquinazol C	24.7	-5.9	123.6	-3.3	3.2	-1.8	-3.8	29.8	-0.9	-3.6	-4.5	-5.1	-3.7	-6.8
11	2”-Oxovoruscharin		-7.5		157.2	288.5		25.2	353.8	282.1	135.3		-7.2	88.4	-9.5
12	Liquiritigenin	10.2	-7.1	70.4	-4.1	-3.5	-3.8	-4.9	2.8	-3.7	-4.2	-4.8	-5.8	-7.7	-6.9
13	4H-Pyran-4-one,2,3-dihydro-3,5-dihydroxy-6-methyl-	-3.3	-4.6	16	-3.2	-3.3	-3.5	-4.4	-3.1	-3.2	-3	-3.5	-3.8	-6	-4.4
14	Heneicosanal	7.2	-5.4	32.6	-3.5	-2.9	-3.3	-2.5	2.4	-0.3	-2.8	-3.3	-3.3	-6.4	-4.4
15	Frugoside	157.6	-6.8	273.4	12.4	78.3	66.3	-2.9	183.2	47.3	1.9	12.5	-5.6	10.9	-8.3
16	Coroglaucigenin	84.5	-6.4	229	-2	45.2	31	-3.8	87.3	44.7	-3.3	-4.6	-5.5	6.9	-7.2
17	(-)-Globulol	13.5	-5.5	57.5	-3.8	-2	-2.2	-4.6	4.6	0.2	-3.3	-4.8	-4.7	-1.9	-6
18	1,1,6,6-tetramethyl-cyclodecan	7.6	-5.1	50.3	-3.2	-2.2	-2.3	-3.7	3.3	-1	-2.8	-4.7	-4.3	-4.2	-5.6
19	1-Eicosanol	5.6	-5.4	34.8	-3.9	-2.7	-3.1	-2.7	1.5	-1.5	-3	-3.3	-4	-6.2	-4.5
20	Docosane	8.7	-5.7	38.9	-3.5	-2.2	-3.1	-2.5	4.9	-0.8	-2.8	-3.4	-3.3	-6	-4.8
21	Nonacosane	19.6	-5.7	57.6	-3.3	0.1	-2.1	-2.7	13.8	1.5	-2.9	-3	-3.5	-4.9	-4.6
22	Tritriacontane	34.8	-5.6	61.2	-2.7	4.9	-2.2	-2.1	24.2	6.8	-3	-3.2	-3.1	-2.6	-4.5
23	Tamarixin	57.7	-6.1	128.6	-3.4	28.8	6.8	-3.7	66.6	32.5	-3.2	-5.2	-5.1	3	-7.1
24	Glutathione	4.2	-5.2	25.5	-3.8	-3.2	-3.4	-4	-2.3	-2.8	-3.5	-3.5	-4.3	-7.1	-5.1
25	Tricosane	9.5	-5.6	39.7	-3.2	-2	-2.9	-2.6	7.2	-0.3	-2.8	-3.2	-2.9	-6.4	-5
26	Cyanidin	8	-5.9	119.8	-3.9	1.6	0.1	-4.2	13.4	-1.6	-4.4	-5	-5.3	-6.6	-6.8
27	8-Pentadecanone	3.5	-5.7	20.7	-3.6	-3.2	-3	-2.9	-1.8	-2.1	-3	-3.2	-3.5	-6.1	-4.8

28	Armillane	49.6	-6.4	126.3	-3	6.5	5.1	-4.7	39.6	14.4	-3.3	-5	-5.9	-4.2	-8.1
29	1-[2,4-dihydroxy-3-[(2S,3R,4R,5S,6R)-3,4,5-trihydroxy-6-(hydroxymethyl) oxan-2-yl]phenyl]-3-hydroxy-3-(4-hydroxyphenyl)propan-1-one	29	-7	74.3	-4.1	-1.6	-4.6	-4.9	23.8	-2	-4.2	-5.3	-5.4	-5.5	-7.2
30	2-Cyclopenten-1-one	-3.3	-3.8	4.7	-2.5	-2.4	-2.6	-3.1	-2.7	-2.3	-2.3	-2.5	-2.9	-4.1	-3.6
31	Taraxasterol acetate	278.6	-7.4		40.9	173.1	136.8	-2.4	179.2	127.7	3.5	49.9	-6.4	32.2	-9
32	Calotropagenin	118.8	-6.6		0	85.1	40.6	-2.7	100.5	53.3	-3.1	-1.6	-5.6	9.8	-7.4
33	Germanicol acetate	253.9	-7.7		26.9	160	93.8	-3.1	146	155.3	9.4	41.5	-6.4	21.2	-8.9
34	1-tetradecene	-1.3	-4.9	14.1	-3.7	-2.9	-2.9	-2.6	-2.5	-1.5	-2.8	-3	-3.2	-5.6	-4.5
35	1-Heptadecanol	3.1	-5.3	19.3	-3.7	-3.1	-3.3	-2.6	-1.1	-1.6	-2.9	-3.4	-3.7	-6	-4.8
36	15 β-Hydroxycalotropin	422.1	-6.4		101.9	230.5	228.3	4.1	263.9	176.2	28.2		-6.4	49.2	-9
37	Gigantursenyl acetate B	200.3	-7.9		17.9	162.7	87.6	-3	145.3	107	-0.2	111.2	-6.4	28.7	-8.8
38	Giganticine	6.3	-5.8	69	-4.1	-3	-2.4	-3.7	1.3	-2.3	-3.9	-3.9	-4.8	-6.6	-6.6
39	Decane	-3.8	-4.8	6.8	-3.2	-2.5	-2.5	-2.6	-2.3	-1.6	-2.4	-2.6	-3.5	-4.9	-4.4
40	9,10-Epoxystearic acid	7.9	-5.8	32.6	-3.9	-3.4	-3.3	-2.9	1.4	-1.7	-3.6	-3.8	-3.7	-7.1	-5.3
41	Calotropin	432.1	-6.4		98.7	202.1	233.9	3.6	244.3	178.1	16.7		-6.3	28.3	-9
42	Curcumenol	9.4	-5.8	73.2	-3.9	-1.9	-2.1	-4.4	4.9	-0.3	-3.5	-4.9	-5.1	-5.6	-6.6
43	Campesterol	-6.3	-8.5	-7	-6.9	-7	-7	-7	-5.3	-5.4	-5.9	-8	-5.9	-6.9	-8
44	Pentadecanal	2.9	-5	17.7	-3.8	-3.4	-3.3	-2.7	-1.6	-1.8	-2.7	-3.4	-3.3	-5.8	-4.6
45	Chlorogenic acid	22.2	-6.1	64.6	-4.1	-0.4	-4.3	-4.6	9.3	-0.8	-4.1	-4.9	-5.4	-8	-7.3
46	Tacrine	0.7	-6.4	39.5	-3.8		-4.3	-4.5	-1	-2.5	-3.4	-4.9	-4.9	-6.5	-6.3
47	Diisooctylphthalate	-3.8	-5.6	24.6	-3.6	-4.1	-3.7	-4.9	-2.7	-2.7	-3.5	-4.3	-4.4	-7.2	-6.4
48	Sapogenins	162.5	-7.8		22.9	139.3	80.8	-3.5	159.3	75.1	-1.3	9.1	-7.4	22.6	-9.3
49	Methyl 14-methylpentadecanoate	4.3	-5.4	29.1	-3.8	-2.9	-3.2	-3	-0.4	-1.5	-2.8	-3.5	-4	-6.6	-4.9
50	5,12-Naphthacenedione, 8-ethyl-7,8,9,10-tetrahydro-1,6,10,11-tetrahydroxy-,(8R-cis)-	29.8	-7	156.8	-3.8	20.9	-3	-4.3	63.9	17.8	-4.2	-6	-5.9	6.1	-8.1
51	Benzoic acid	-4.1	-4.9	8.3	-3.2	-3.3	-3.8	-3.9	-3.3	-2.6	-3.2	-3.5	-4.1	-5.8	-4.8
52	Bumetanide	20.4	-5.6	60.5	-3.5	-3.6	-2.4	-4	9.1	1.2	-2.8	-4	-4.6	0.9	-6
53	Gofrusid	170.1	-7.8		10.5	96.3	114.1	-3	136.8	98.3	3.3	44.6	-6.4	9.8	-8.3
54	Lupeol	-6.9	-8.2	-7.1	-7.1	-7.1	-7.1	-7	-6.1	-6	-6.1	-9.5	-6.2	-7.8	-8.5
55	1-Hexadecanol	2.9	-5.5	17.1	-4	-3.3	-3.3	-2.6	-1.8	-1.6	-2.8	-3.5	-3.5	-6	-4.5

56	Digoxin	192.8	-6.3		27.9	138.3	66	1.2	184	126.9	2.6	21.6	-6.9	40.8	-9
57	1-Nonadecene	5.1	-5.7	29.3	-3.3	-2.8	-3.1	-2.5	-1.2	-1.3	-2.9	-3.4	-3.1	-6	-5.1
58	Octadecane,3-ethyl-5-(2-ethylbutyl)-	11.7	-5.3	55.2	-3.5	-1	-2.8	-2.6	11.2	0.1	-2.4	-3.3	-3.7	-4.7	-4.7
59	Oxadiazon	29.5	-5.7	98.3	-3	-1.9	-1.7	-3.8	20.4	-0.4	-3.7	-4.7	-5.2	-5.8	-7.2
60	Calotroposide A	324.6	-5.5		106.6	226.5	107.3	9.5	282.9	255.5	38.9	162.2	-5.9	115.2	-9.1
61	Ethyl hexanoate	-4.3	-4.5	6.5	-3.3	-3	-2.9	-3	-2.8	-2.3	-2.9	-2.9	-3.3	-5.1	-4.5
62	Isoamyl acetate	-4.5	-4.3	6.1	-3	-2.9	-2.8	-3.1	-2.9	-2.6	-2.8	-2.9	-3.2	-5	-4.5
63	desglucouzarin	165.2	-7		4.3	100.1	62.9	-3.9	149.3	89	-0.2	-0.7	-6.1	2.4	-8.7
64	Ethion	7.2	-4	47	-3.2	-3	-2.5	-2.7	9.3	-0.9	-2.6	-3.2	-3.2	-5.2	-4.1
65	(4,4,6a,6b,8a,11,11,14b-Octamethyl-1,2,3,4a,5,6,7,8,9,10,12,12a,14,14a-tetradecahydropicen-3-yl)acetate	203.5	-7.3		36.6	120.1	75.1	-3	194	81	-2.3	43.5	-6.8	25.8	-8.8
66	Isovalerate	-3.8	-3.9	3.5	-2.8	-2.7	-3.1	-3	-2.9	-2.4	-2.5	-2.6	-3	-4.5	-3.9
67	Ibogamine,12-methoxy-	42.9	-6.6	130.9	-4.5	-2.2	-0.6	-4.2	26.7	-0.1	-3.2	-5.8	-5.7	-1.2	-7.1
68	Gallic acid	-3.4	-5	16.5	-3.4	-3.8	-3.4	-4.9	-2.9	-3	-3.3	-3.8	-3.9	-6.2	-5.1
69	Octanoic acid	-4.2	-4.9	6.1	-3.4	-3.2	-3.1	-3.4	-3.4	-2.6	-2.9	-3.3	-3.7	-5.3	-4.6
70	Kojic acid	-3.7	-4.6	9.2	-3.3	-3.5	-3.4	-4.1	-3.1	-3	-3	-3.6	-3.5	-5.4	-4.6
71	Profenofos	8.3	-4.7	42.4	-3.2	-2.7	-2.4	-3.4	9.3	-2.5	-3.2	-4.2	-3.8	-5.7	-4.9
72	Metamitron	-3	-6.3	31	-3.9	-3	-4.2	-4.3	-0.6	-2.4	-3.8	-4.9	-4.8	-7.8	-6.4
73	Acarbose	62.8	-5.3	143.8	-1.8	27.9	6.8	-4.2	77.8	29.8	-1.7	-2.8	-5.3	2.3	-6.9
74	Emmotin A	11.4	-5.6	49.6	-3.5	-2.6	-3.6	-3.9	8.8	-1.5	-3.4	-4.5	-4.7	-0.5	-6.5
75	Ouabain	194.1	-6.2	259.1	10.4	98	49.9	-0.9	136.2	76.2	8.3	20.8	-5.7	5.3	-7.8
76	Asclepin	351.8	-7		80.4	197.4		3.2	237.5	134.2	7.8		-6.2	29.1	-8.8
77	Calactin	247	-6.8		29.5	144.1	88.4	-3.6	205.7	76.4	-1.4	62.2	-6.9	22.6	-8.5
78	Uscharidin	510.8	-7.3		100.5	214.2	327.4	2.3	279.3	142.2	11.1		-6.5	47.9	-9.2
79	Levomenol	0.9	-6.4	27.8	-3.8	-3.2	-2.9	-3.6	-1.4	-1.3	-3.3	-4.5	-5.1	-7.7	-6
80	Gingerol	8.8	-6	40.4	-4.4	-2.8	-3.4	-3.8	-0.6	-3	-3.8	-4.1	-4.4	-7.6	-5.8
81	Elaeokanine C	0	-4.8	33	-3.9	-2.6	-2.9	-3.6	-1.4	-1.4	-3.5	-3.9	-4.1	-5.4	-5.5
82	Voruscharin	373.3	-6.6		92.9	174.5	150.6	-2.6	239.2	155.7	12.6		-6.9	30	-9.3
83	Cinnamic acid	-4.4	-5.3	15.9	-3.5	-2.9	-3.1	-3.8	-3.3	-2.6	-3.5	-3.7	-4.5	-6.4	-5.7
84	Palmitoleic acid	2.6	-5.3	23.1	-4.3	-3.8	-3.4	-3.2	0	-1.7	-3.4	-3.9	-4.1	-6.6	-5.1
85	Oleic acid	4.5	-5.5	26.8	-4	-3.6	-3.3	-2.7	-0.1	-1.8	-3	-3.9	-4.2	-6.7	-4.8

86	Ferulic acid	-2.8	-5.3	20.8	-3.6	-2.7	-3.2	-4.3	-2.4	-2.5	-3.5	-3.8	-4.3	-7.1	-5.5
87	Benalaxyl	29.1	-5.2	67.3	-3.1	1.2	1	-4	14.4	-0.8	-3.3	-5	-5.3	-2.8	-6.5
88	Tetrapentacontane	76.9	-4.1	121.2	7.1	67	11.1	-1.4	74.1	60.7	-2	18.6	-3.1	19.8	-4.4
89	Acacetin	10.9	-6.1	114.3	-3.8	33.7	-3.7	-4	29.5	4.9	-4.4	-4.8	-5.5	-6.8	-7.3
90	Linoleic acid	4.9	-5.7	26.7	-3.9	-2.4	-3.5	-2.8	1.7	-1.7	-3.1	-3.8	-3.5	-7	-5.1
91	Stigmasterol	-7	-8.5	-7	-7	-6.9	-7	-7.3	-5.6	-5.7	-5.6	-8.5	-6.2	-8	-8
92	Rutin	-7.6	-8.7	-7.2	-7.2	-7.2	-7.2	-7.1	-5.9	-6.1	-6	-8.9	-6.2	-11.5	-8.2
93	Linolenic acid	3.6	-6	29.7	-3.9	-3	-3.4	-3.2	0.6	-1.3	-3.3	-4.2	-4	-7.3	-5.5
94	Hyperoside	62.2	-5.2	132.8	-3.6	59.4	-3.2	-4	49.6	-1	-3.9	-3.3	-5.3	2.7	-7.4
95	Stearic acid	3.7	-5.3	27.4	-3.8	-2.8	-3.2	-2.8	0	-1	-3	-3.7	-4.1	-6.5	-4.8
96	Ethyl linoleate	8.9	-5.9	38.7	-3.8	-0.9	-3.1	-2.9	1.3	-1.3	-3.4	-3.5	-3.6	-7	-5.3
97	Cis-vaccenic acid	3.8	-5.5	29.2	-3.8	-2.6	-3.4	-3	0.1	-2.9	-3.2	-3.5	-3.6	-6.8	-5.1
98	Methyl linoleate	5.9	-6.1	29.1	-3.6	-2.1	-3.5	-2.9	1.1	-3	-2.9	-3.6	-4	-6.9	-5.1
99	Propane-1,3-diamine,N,N′-bis(3-ethoxy-1-methyl-3-oxo-1-propenyl)-	8.7	-5	32.4	-3.8	-1.9	-3.5	-3.3	-0.2	-2.5	-3.3	-3.8	-3.7	-7.2	-5.6
100	5,8,12-Trihydroxy-9-octadecanoic acid	9.4	-5.8	37.6	-4.2	-1.6	-3.5	-3.5	2.3	-3.2	-3.4	-3.4	-3.9	-7.4	-5.4
101	Batatifolin	18.3	-5.7	124.2	-4	44.5	-3.3	-3.6	34.9	-2.9	-4.3	-5.2	-5.2	-6.1	-7.3
102	Beta-Sitosterol acetate	102.4	-7.6	219.6	-1.6	76.6	-1.5	-4.1	82.2	15.6	-3.6	-4.1	-6	5.2	-8.3
103	Ethyl oleate	8.4	-5.2	33.2	-3.6	-0.4	-3.3	-2.8	0	-2.3	-2.9	-3.7	-3.3	-6.7	-5.1
104	1-(3-([[(2E)-5-(3,3-Dimethyl-2-oxiranyl)-3-methyl-2-pentenyl]oxy) phenyl)ethanone	10.9	-6.6	43.2	-4.3	-3.3	-4.1	-4	5.1	-3	-4.1	-4.8	-4.8	-8	-6.6
105	Z-1,6-Tridecadiene	-2.1	-5.1	12.4	-3.6	-2.8	-2.6	-2.8	-2.5	-2.7	-2.1	-3.2	-3.5	-5.6	-4.9
106	Trielaidin	85.6	-4	106.2	12.6	74.5	13.9	-1.2	85.3	39.4	-1.9	17.4	-3.4	24.5	-5.4
107	(E)-3-Octadecene	3.9	-5.6	20.8	-3.4	-2.3	-3.3	-2.6	0	-2.3	-2.9	-3.3	-3.8	-6.3	-4
108	1,6,10,14,18,22-Tetracosahexaen-3-ol,2,6,10,15,19,23-hexamethyl-,(all-E)-	40.1	-7.8	87.8	-3.8	5	-2.9	-3.3	39.7	-0.3	-3.6	-2.6	-4.7	-5.9	-6.9
109	5-Nonadecen-1-ol	3.5	-5.5	32.4	-4	-2.2	-3.5	-2.6	1.5	-2.6	-2.9	-3.6	-3.4	-6.3	-4.8
110	2,4-Dihydroxy-2,5-dimethyl-3(2H)-furanone	-3.8	-4.6	17.1	-3.4	-3	-3.2	-3.8	-3.3	-2.9	-3.2	-3.6	-3.9	-6	-4.8
111	8-tetradecyn-1-ol acetate	2.9	-5.6	28.6	-4.3	-2.7	-3.3	-3.1	-1	-2.9	-3.5	-3.8	-3.9	-6.6	-5.1
112	Ascorbic acid	-4.2	-4.6	12.3	-3.3	-3.3	-3.4	-4.6	-2.9	-3.5	-3.8	-3.5	-3.8	-6.2	-4.5

113	Pyrrolidine-2-carboxamide	-3.8	-4.3	6.4	-2.8	-3	-3.6	-3.6	-2.9	-2.8	-2.6	-3.1	-3.3	-5.2	-4.1
114	Methyl 17-methyloctadecanoate	8.1	-5.6	32.5	-3.5	-1.1	-3.1	-2.7	4.8	-2.4	-2.8	-3.2	-4.1	-6.8	-5.1
115	2-Pyrrolidinone,5-(cyclohexylmethyl)-	-2.7	-5.8	20.2	-3.7	-3.4	-3.5	-3.9	-3	-3.1	-3.3	-4	-4.4	-6.9	-5.1
116	2-[3-Carbethoxy propionamide]-3,4-dicarbethoxy-1-benzyloxy methyl pyrrole	33.4	-6.3	66.7	-3.8	17.9	-3.1	-3.8	49.7	-2.7	-3.2	-3.6	-4.5	-3.8	-6.7
117	Cyclohexane,1,1'-(oxydi-2,1-ethanediyl)bis[4-methyl-	11	-6.9	39	-4.4	-2.4	-3.9	-3.2	1.6	-2.9	-3.9	-4.2	-3.7	-7.2	-5.2
118	Cyclohexanamine,3,6-diethenyl-2,2-dimethyl-N-(2-methylpropylidene)-	9.8	-5.2	47.9	-3.2	-2	-2.7	-3.5	6.1	-2.4	-2.9	-4.3	-4.1	-4.7	-5.7
119	Urs-12-ene	157.8	-7.9	477.5	4.7	171.2	24.7	-3	169.9	46	-3.7	-0.6	-6.9	25.8	-8.4
120	L-ornithine	-4.1	-4	5.2	-2.7	-3.2	-3.2	-3.6	-2.8	-2.9	-3	-3.2	-3.2	-4.6	-3.8
121	ethylene	-1.7	-1.9	-0.8	-1.3	-1.2	-1.2	-1.3	-1.3	-1.1	-1.1	-1.2	-1.5	-1.9	-1.8
122	Squalene	28.8	-7.1	89.9	-4.1	9.1	-2.8	-2.9	32.8	-0.5	-4	-4	-4.4	-6.1	-6.5
123	2,2-Dimethylbutane	-2.4	-3.5	4.6	-2.3	-2.2	-2.6	-2.6	-2.5	-1.9	-2	-2.3	-2.9	-3.8	-3.6
124	Sulfurous acid, nonylpentyl ester	2.7	-5.3	19	-3.6	-3.2	-3.2	-3	2	-3	-3.1	-3.5	-3.6	-6.3	-5.1
125	Trans-Linalool oxide	-2.9	-4.8	23.4	-3.3	-2.9	-3.2	-3.6	-2.9	-3.1	-3.3	-3.5	-3.7	-6.5	-5.2
126	29-Methylisofucosterol	82.3	-8.6	172.6	-2.5	59.2	-2.1	-3.4	53.3	6.5	-4	-4.8	-6.1	-0.9	-8.5
127	Isoprene	-3.2	-3.5	2.2	-2.2	-2.3	-2.4	-2.5	-2.5	-1.9	-2	-2.2	-2.8	-3.4	-3.5
128	Nonic acid	-3.9	-4.9	10.3	-3.4	-3.1	-3.8	-3.9	-2.9	-3.1	-3.5	-3.5	-3.6	-5.9	-5.2
129	Isobergapten	2.3	-5.6	34.3	-3.6	-2.8	-3.9	-4.2	-0.8	-3	-3.5	-4.5	-4.5	-4.8	-5.9
130	Dehydrovomifoliol	20.9	-5	47	-3.3	1.4	-3.6	-3.8	1.8	-1.9	-3.1	-4.4	-4	-4.7	-5.7
131	Caffeic acid	-3.5	-5.5	18.5	-3.5	-2.4	-3.7	-4.5	-1.6	-3.1	-3.6	-3.7	-4.3	-7.5	-5.8
132	1-Triacontanol	27.8	-5.5	59.6	-3.3	6.2	-2.1	-2.5	33.7	0	-2.5	-3	-3.2	-4.2	-4.5
133	11-Oxo-A-amyrin	175.1	-7.2		9.7	187.8	22.9	-4	180.8	36.6	-3	12.3	-6.5	17.9	-9.5
134	Bicyclo[4.2.0]octa-1,3,5-triene	-3.5	-4.8	9.9	-3	-3	-2.9	-3.6	-2.9	-2.4	-2.6	-3.3	-4.1	-5.1	-4.9
135	calotropone	82.7	-6.8	178.3	-1.5	76.3	7.6	-3.8	92.3	6.5	-2.8	-5.2	-5.9	8.2	-8.5
136	Biphenyl	-3.2	-6	22.1	-3.8	-2.4	-3.5	-4	-2.5	-3.1	-3.1	-4.1	-5.5	-6.8	-6.1
137	(-)-Epicatechin	12.7	-6.9	88.6	-3.8	5.8	-3.3	-4.4	28.7	-3.1	-4.1	-5	-5.4	-7	-6.7
138	β-Amyrin	-7.4	-8.9	-7.4	-7.4	-7.5	-7.5	-7.6	-6.1	-6.7	-6.1	-9.5	-6.9	-8.9	-8.6
139	α-Amyrin	164.6	-6.7	218.1	0.1	75	23.9	-4	151.3	22.4	0.6	12.2	-6.4	43.4	-8.3

140	Deidaclin	1.4	-5	31.6	-2.9	-1.9	-3.9	-4.9	-1.2	-3.1	-3.6	-4.3	-4	-6.1	-6.1
141	Furfuryl alcohol	-4	-3.9	1.8	-3	-3	-3.3	-3.2	-3	-2.5	-2.7	-3.1	-2.9	-4.6	-3.9
142	2-Amino-2-Deoxy-Hexose	-2.7	-4.2	15.2	-3.5	-2.5	-3.2	-4.3	-2.4	-3.3	-3	-3.8	-3.6	-5.9	-4.7
143	Thiosulfuric acid(H2S2O3),S-(2-aminoethyl)ester	-3.5	-3.5	6.1	-3.1	-2.7	-2.8	-3	-2.6	-2.8	-2.8	-3	-3	-4.7	-3.6
144	3,7-Dimethyloctan-1-ol	-3.2	-4.7	9.2	-3.3	-2.9	-3.4	-3.1	-3	-2.8	-2.9	-3.4	-4	-5.5	-4.5
145	Methoxyacetaldehyde diethyl acetal	-2.7	-3.8	6.8	-2.9	-2.3	-2.8	-2.7	-2.6	-2.7	-2.6	-2.6	-2.7	-4.7	-3.9
146	Cyclohexane	-2.2	-3.8	6.7	-2.4	-2.1	-2.3	-2.9	-2.3	-2	-2	-2.5	-3	-3.8	-3.6
147	Piperidine	-2.9	-3.6	4.8	-2.4	-2.3	-2.3	-2.9	-2.3	-2.1	-2.1	-2.5	-2.6	-3.8	-3.4
148	1-Octene	-3.9	-4.5	5.1	-2.9	-2.3	-2.5	-2.7	-2.4	-2.3	-2.1	-2.4	-3.4	-4.3	-4.1
149	1-Undecanol	-3.3	-4.8	8.8	-3.5	-3	-3.1	-2.8	-2.5	-2.9	-2.6	-3.4	-3.7	-5.4	-4.3
150	1-Tetradecanol	0.1	-5.1	14.5	-3.7	-3.1	-3.2	-2.9	-1.6	-2.7	-2.6	-3.2	-3.4	-5.7	-4.5
151	Eicosane	4.4	-4.9	28.1	-3.7	-1.1	-3	-2.4	1	-2.1	-2.2	-3.3	-3.6	-6.4	-4.4
152	Propylene	-2.4	-2.7	-1	-1.8	-1.8	-1.7	-1.9	-1.7	-1.5	-1.6	-1.5	-2	-2.5	-2.5
153	Isobutylene	-2.7	-3.1	0.2	-1.9	-2	-2	-2.2	-2.1	-1.6	-1.9	-1.9	-2.3	-2.9	-3.1
154	N,N-Bis(2-hydroxyethyl) dodecanamide	3.9	-5.1	28.6	-3.7	-2.1	-3.2	-3.5	1.8	-2.8	-3	-3.6	-3.7	-6.3	-5.2
155	Methyl 8,11,14-Heptadecatrienoate	4	-6.2	29.9	-4.1	-1.8	-3.4	-2.9	1.1	-2.8	-2.8	-3.5	-4.3	-7.4	-5.2
156	Isoavocadienofuran	2.8	-6.3	24.9	-4.3	-2.9	-3.2	-3	-1.8	-2.7	-2.9	-3.5	-4.4	-6.9	-4.9
157	Lupeol acetate	182.7	-7.1		11.9	192	20.3	-3.3	170.7	34.6	-3.8	5.4	-6.1	17.3	-8.4
158	Azulene	-2.7	-5.4	19.9	-3.4	-3	-3.2	-3.8	-2.9	-2.8	-3.1	-3.7	-4.6	-6.1	-5.3
159	Uzarigenin	106.3	-6.7	199.9	-2.6	94.4	3.6	-3.1	123	11.9	-3.7	-4.5	-5.9	8.9	-7.7
160	2-hydroxyhexadecanoic acid	2.7	-5.5	22.1	-4.1	-3	-3.6	-3.2	-0.9	-3	-2.9	-4	-3.9	-6.6	-5.3
161	2-(1-Phenylethyl)phenol	-0.7	-7.1	28	-4.4	-2.3	-3.8	-4.5	-2.3	-3	-3.8	-4.6	-5.5	-7.2	-6.1
162	2-Hexyl-1-decanol	2.8	-5.6	22.3	-3.5	-2.3	-3.1	-2.9	-1.3	-2.4	-2.6	-3.4	-3.4	-6.4	-4
163	Palmitic acid	2.7	-5.4	20.4	-3.9	-2.4	-3.3	-2.8	-1.2	-2.6	-2.7	-3.6	-3.9	-6.4	-4.6
164	Benzoyllineolone	96.2	-6.8	160.6	-3.4	72.5	-0.5	-4.4	106.2	11.5	-4.2	-3.2	-6.5	7.9	-8.3

PLA_2 - Phospholipase A_2, COT – Cobratoxin, LN1 – Long neurotoxin 1, LN2 – Long neurotoxin 2, LN3 – Long neurotoxin 3, LN4 – Long neurotoxin 4, LN5 – Long neurotoxin 5, CA – Cobramine A, CB - Cobramine B, CYT 3 – Cytotoxin 3, PL – Proteolase, SP – Serine protease, L-AAO – L-Amino acid oxidase, AchE – Acetylcholine esterase

Lupeol and β-amyrin showed inhibitory activity against all 14 targets, while rutin inhibited 13 targets except cobramin A. Except for cobramin A, cobramin B, and cytotoxin 3, all other 11 targets were inhibited by stigmasterol. Similarly, campesterol inhibited 10 targets, excluding cobramin A and B, cytotoxin 3, and serine protease. The compound 2,4-bis(1-phenylethyl)phenol exhibited inhibitory activity against five targets: cobramin, proteolase, serine protease, L-amino acid oxidase, and acetylcholinesterase. A total of 37 compounds inhibited three targets; 25 compounds inhibited cobratoxin, serine protease, and acetylcholinesterase, and 11 compounds inhibited cobratoxin, L-AAO, and acetylcholinesterase. The left-over compound, 5,12-naphthacenedione 8-ethyl-7,8,9,10-tetrahydro-1,6,10,11-tetrahydroxy-8R-cis, had inhibited the targets cobratoxin, proteolase, and acetylcholinesterase.

Among the 21 phytochemicals that exhibited inhibition against two targets, ten were effective against cobratoxin and acetylcholinesterase, while five inhibited LAAO and acetylcholinesterase. The remaining six compounds—gingerol, linoleic acid, methyl linoleate, cyclohexane, 11-(oxydi-2,1-ethoxy-1-methyl)-bis [4-methyl], methyl 8,11,14-heptadecatrienoate, and isoavocadienofuran—showed inhibitory activity against cobratoxin and L-AAO. Based on the binding score and multiple target binding affinity analyses, five molecules—campesterol, lupeol, stigmasterol, rutin, and β-amyrin—were identified for lead optimization. Among these compounds, lupeol and β-amyrin exhibited inhibitory activity across all 14 selected cobra venom targets. Rutin demonstrated binding energies lower than -6 kcal/mol with all targets except cobramin A; for cobramin A, the binding energy was -5.9 kcal/mol. Despite this, rutin can still be considered a lead with inhibitory potential against all targets. Campesterol showed binding scores of -5.3 kcal/mol with cobramin A, -5.4 kcal/mol with cobramin B, and -5.9 kcal/mol with cytotoxin 3 and serine protease, with binding scores below -6 kcal/mol for the remaining targets. Similarly, stigmasterol exhibited binding scores of -5.6 kcal/mol with cobramin A, -5.7 kcal/mol with cobramin B, and -5.6 kcal/mol with cytotoxin 3, while binding scores for all other targets were lower than -6 kcal/mol. Consequently, stigmasterol can also be considered for lead optimization. Table 2 illustrates the hydrogen bond (H-bond) and hydrophobic interactions between 14 selected cobra venom targets and two phytochemicals with medium to high binding energies across these targets. Among these targets, lupeol formed H-bonds with PLA_2 and SP, while β-amyrin showed H-bond interactions with AchE and cobramin B. Both ligands displayed only hydrophobic interactions with the remaining targets. H-bonds contribute to binding specificity and stability, especially at shorter distances, which indicate stronger interactions.[40] Hydrophobic (non-polar) interactions, although less specific, also contribute to binding energy and stability. Effective ligand binding typically involves both hydrogen bonding and hydrophobic stabilization.[41] Based on this interaction profile, β-amyrin emerges as a promising lead ligand due to its robust and specific binding characteristics across multiple targets. Its short, stable H-bonds with key residues in AchE and cobramin B enhance affinity, while its consistent hydrophobic interactions further stabilize binding in non-polar environments. This blend of H-bonding and hydrophobic interactions indicates that β-amyrin is a potential lead compound, showing superior affinity and stability compared to ligands that lack these features. The docked complexes of 14 selected cobra venom proteins with leads such as β-amyrin and lupeol are presented in Figs 1A-N and 2A-N, respectively.

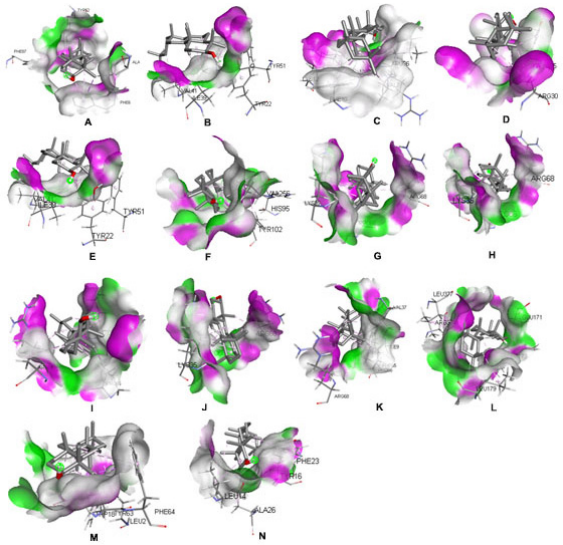

Fig. 1: Docking interactions of the ligand β-Amyrin with: A. Acetylcholinesterase, B. Cobramin A, C. Cobramin B, D. Cobrotoxin, E. Cytotoxin 3, F. L-Amino Acid Oxidase, G. Long Neurotoxin 1, H. Long Neurotoxin 2, I. Long Neurotoxin 3, J. Long Neurotoxin 4, K. Long Neurotoxin 5, L. Protease, M. Phospholipase A2, and N. Serine Protease.

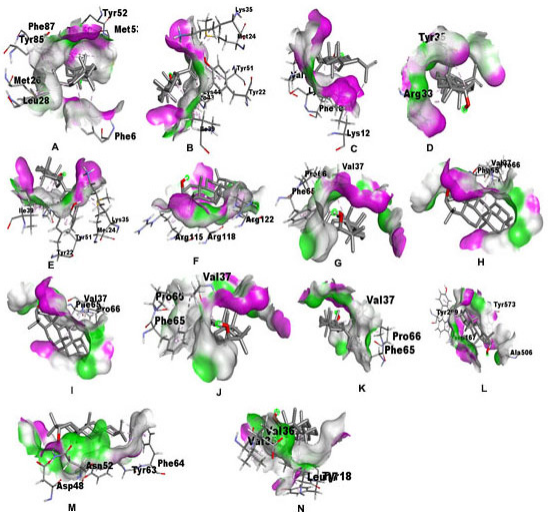

Fig. 2: Docking interactions of the ligand Lupeol with: A. Acetylcholinesterase, B. Cobramin A, C. Cobramin B, D. Cobrotoxin, E. Cytotoxin 3, F. L-Amino Acid Oxidase, G. Long Neurotoxin 1, H. Long Neurotoxin 2, I. Long Neurotoxin 3, J. Long Neurotoxin 4, K. Long Neurotoxin 5, L. Protease, M. Phospholipase A2, and N. Serine Protease

Table 2: The hydrogen bond and hydrophobic interaction between the ligands, lupeol and β-amyin with the selected 14 cobra venom proteins

Proteins	*Ligands*	*Hydrogen bonds*	*Distance (Å)*	*Hydrophobic interaction*
AchE	Lupeol	Nil	Nil	LEU28,MET53,LEU28,MET26,PHE6,TYR52,TRP58,TYR 85,PHE87
CA		Nil	Nil	ILE39,LYS44,MET24,LYS35,PRO43,TYR22,TYR51
CB		Nil	Nil	LYS5,VAL7,LYS12,PHE10
COT		Nil	Nil	ARG33,TYR35,
CYT3		Nil	Nil	ILE39,LYS44,MET24,LYS35,PRO43,TYR23,TYR51
L-AAO		Nil	Nil	LEU128,ARG115,ARG118,ARG122
LN 1		Nil	Nil	PRO66,VAL37,PHE65
LN 2		Nil	Nil	VAL37,PRO66,PHE65
LN 3		Nil	Nil	VAL37,PRO66,PHE66
LN 4		Nil	Nil	VAL37,PRO66,PHE65
LN 5		Nil	Nil	VAL37,PRO66,PHE65
PL		Nil	Nil	ALA506,TRP167,TYR299,TYR573
PLA2		ASP48:OD1---H:Lig	2.21	PHE64, TYR63
		ASN52:HD22---O:Lig	2.4	
SP		VAL36:OD2---H:Lig	3.53	LEU17,VAL35,TYR80
AchE	β-amyin	TYR22:OH---H:Lig	2.18	PHE6,ALA4,TYR52,TRP58,PHE87
CA		Nil	Nil	ILE39,PRO43,VAL41,TYR22,TYR51
CB		ARG36:O---H:Lig	2.01	LEU6,LYS5,VAL7,LYS12,PHE10
COT		Nil	Nil	ARG30,TYR35
CYT 3		Nil	Nil	ILE39,VAL41,PRO43,TYR22,TYR51
L-AAO		Nil	Nil	VAL256,HIS95,TYR102
LN 1		Nil	Nil	PRO66,ARG68,LYS35
LN 2		Nil	Nil	PRO66,ARG68,LYS35
LN 3		Nil	Nil	PRO66,ARG68,LYS35
LN 4		Nil	Nil	PRO66,ARG68,LYS35
LN 5		Nil	Nil	PHE65,VAL37,PRO66,ILE9,ARG68
PL		Nil	Nil	GLU171,LEU377,ARG374,ILE173,LEU179
PLA 2		Nil	Nil	TYR63,PHE64,LEU2,ALA22,TRP18
SP		Nil	Nil	LEU14,ALA26,TYR16,PHE23

ADMET analysis is a prerequisite in drug discovery for forecasting the pharmacokinetic and toxicological profiles of drug candidates, which helps minimize late-stage failures and enhances the overall efficiency of drug development. The pkCSM is an open-access tool for ADMET analysis which can predict the pharmacokinetic and toxicological properties of ligands with high accuracy and efficiency.[6] Hence, the ADMET analysis was done using this tool and the results are shown in Table 3.

ADMET properties of the strongly binding leads β-amyrin and lupeol with all the selected targets indicate that both compounds have poor water solubility, with β-amyrin being slightly less soluble. They share similar Caco2 permeability and intestinal absorption rates, with lupeol being marginally higher. These are not substrates but inhibitors of p-glycoprotein, potentially impacting drug transport and absorption. While β-amyrin has a lower volume of distribution (VDss), both compounds are highly plasma protein-bound and demonstrate moderate BBB permeability, with lupeol slightly higher.

In terms of metabolism, both compounds are substrates for CYP3A4 but do not inhibit other major CYP enzymes,

Table 3: ADMET analysis of lupeol and β-amyrin using pKCSM

Properties	*β-Amyrin*	*Lupeol*
Water solubility	-6.531	-5.861
Caco2 permeability	1.226	1.226
Intestinal absorption (human)	93.733	95.782
Skin Permeability	-2.811	-2.744
P-glycoprotein substrate	No	No
P-glycoprotein I inhibitor	Yes	Yes
P-glycoprotein II inhibitor	Yes	Yes
VDss (human)	0.268	0
Fraction unbound (human)	0	0
BBB permeability	0.667	0.726
CNS permeability	-1.773	-1.714
CYP2D6 substrate	No	No
CYP3A4 substrate	Yes	Yes
CYP1A2 inhibitor	No	No
CYP2C19 inhibitor	No	No
CYP2C9 inhibitor	No	No
CYP2D6 inhibitor	No	No
CYP3A4 inhibitor	No	No
Total clearance	-0.044	0.153
Renal OCT2 substrate	No	No
AMES toxicity	No	No
Max. tolerated dose (human)	-0.56	-0.502
hERG I inhibitor	No	No
hERG II inhibitor	Yes	Yes
Oral rat acute toxicity (LD50)	2.478	2.563
Oral rat chronic toxicity (LOAEL)	0.873	0.89
Hepatotoxicity	No	No
Skin sensitisation	No	No
T. pyriformis toxicity	0.383	0.316
Minnow toxicity	-1.345	-1.696

which indicate the chance of drug-drug interactions is very less. Lupeol has a higher total clearance than β-amyrin, indicating better excretion efficiency. Neither compound is a substrate for renal OCT2 transporters, suggesting limited renal clearance pathways.

β-amyrin and lupeol are non-mutagenic (AMES test) and non-hepatotoxic, showing similar oral toxicity levels in rats. However, their inhibition of hERG II channels could raise concerns about cardiac safety. Overall, despite poor solubility and potential P-glycoprotein interactions, β-amyrin and lupeol demonstrate promising pharmacokinetic profiles with manageable toxicity.

The drug likeness score of both compounds β-amyrin and lupeol show a value of -0.22 which indicates both the compound exhibit drug-like properties.

The MD simulation data reveals that the lupeol-PLA_2 complex (Fig. 3A) demonstrates greater stability compared to the β-amyrin-PLA2 complex (Fig. 3B). The lupeol-PLA_2 complex quickly stabilizes with RMSD values around 1.5 to 2.0 Å, indicating a consistent conformation and strong binding, which aligns with findings on stable ligand-protein interactions.[42] In contrast, the β-amyrin-PLA_2 complex shows higher and more variable RMSD values, reaching up to 3.0 Å, suggesting less stable interactions and possible conformational shifts within PLA_2.[43] These observations imply that lupeol may serve as a more effective stabilizing agent for cobra venom PLA_2, supporting its potential as a more reliable inhibitor.[44]

The RMSF data (Fig 4A & B) suggest that β-amyrin may be a more favorable ligand than lupeol, as it shows lower RMSF values in flexible regions, especially around residues 15, 65, and 80. These lower values indicate that β-amyrin could favorably stabilize the PLA_2 structure, reducing flexibility and enhancing the structural integrity of key regions, which is crucial for effective enzyme inhibition.[45] Stability in these regions typically correlates with improved ligand binding and functional modulation.[46]

The radius of gyration (*Rg*) analysis of cobra venom PLA_2 complexes with lupeol and β-amyrin (Fig. 5A & B) reveals differences in stability over a 100 ns molecular dynamics simulation. The lupeol-PLA_2 complex maintains a stable *Rg* around 1.4 nm with minimal fluctuations, indicating a compact and stable structure that suggests strong binding interactions, likely due to lupeol's stabilizing effect on PLA_2. In contrast, the β-amyrin -PLA_2 complex, while also close to 1.4 nm, shows slightly higher fluctuations, suggesting a comparatively less stable interaction. This difference implies that lupeol may better stabilize PLA2, making it potentially more effective as a ligand in inhibiting PLA_2 activity.

The hydrogen bond interaction data for PLA_2-lupeol (Fig 4A) and PLA2-β-amyrin (Fig 4B) shows a stable bond count, with both fluctuating between 250 to 300 bonds. Lupeol's interaction remains consistent with minor variations, whereas β-amyrin demonstrates a gradual increase in bond count, particularly in the latter half of the simulation. This trend suggests that β-amyrin may establish a progressively stronger interaction with PLA_2, likely due to improved binding or adaptability over time, which has been associated with higher binding affinity in protein-ligand interactions.[47,48] Therefore, while both ligands engage comparably, β-amyrin might achieve a slightly more favorable binding profile due to this increasing hydrogen bond trend.

The simulation results of both lupeol and β-amyrin with PLA_2 revealed that β-amyrin stabilizes flexible regions better (RMSF advantage), lupeol is globally more stable with PLA_2, considering its superior RMSD, compact Rg,

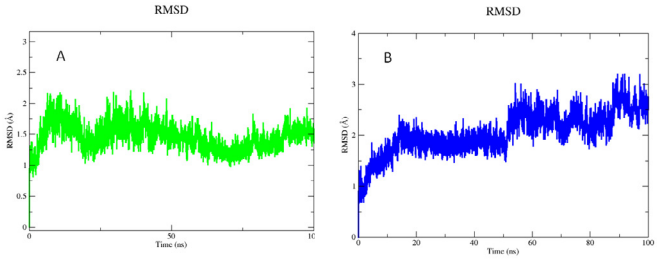

Fig. 3: A & B: MD simulation plot of RMSD. A. cobra venom phospholipase A_2 and lupeol, B. phospholipase A_2 and β-amyrin

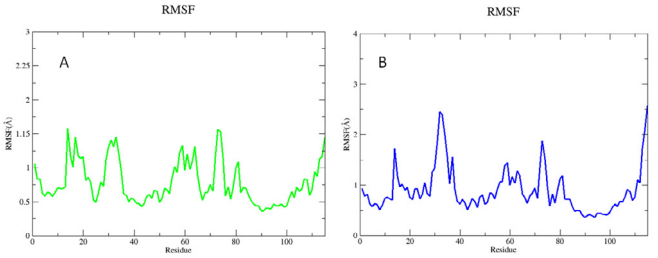

Fig. 4 A&B: MD simulation plot of RMSF. A. cobra venom phospholipase A_2 and lupeol, B. phospholipase A_2 and β-amyrin

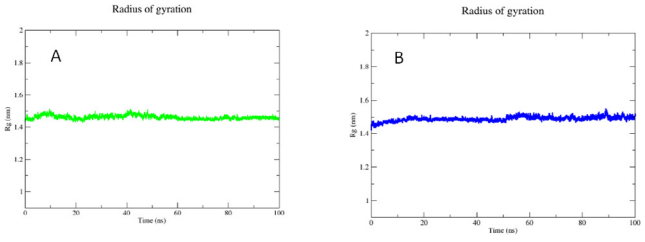

Fig. 5A & B: MD simulation plot of radius of gyration (Rg). A. cobra venom phospholipase A_2 and lupeol, B. phospholipase A_2 and β-amyrin

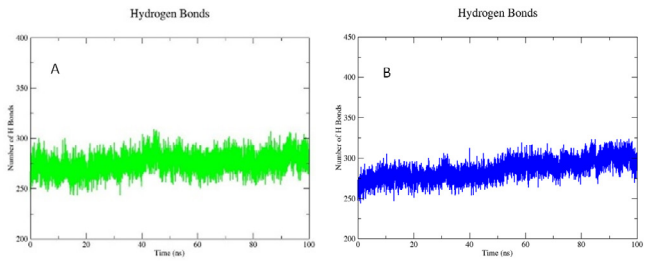

Fig. 6A&B: MD simulation plot of hydrogen bonds' interactions. A. cobra venom phospholipase A_2 and lupeol, B. phospholipase A_2 and β-amyrin

and consistent hydrogen bonding profile. Lupeol is the more stable compound in its interaction with PLA_2 overall. Lupeol and β-amyrin are triterpenoid compounds with notable medicinal properties. Lupeol exhibits a broader range of medicinal properties, such as anti-inflammatory, anticancer, antimicrobial, and hepatoprotective. While β-amyrin has anti-inflammatory, antioxidant, and anticancer properties.[49,50] Lupeol's additional mechanisms, such as apoptosis induction, angiogenesis inhibition and its ability to target multiple pathways in disease processes enhance its therapeutic potential compared to β-amyrin.[51] Thus, lupeol is preferred for its more extensive therapeutic applications. However, the binding score of lupeol and β-amyrin with the selected 14 targets revealed that β-amyrin has a comparatively less binding score than lupeol. In this circumstance, both compounds are suggested for further *in-vitro* and *in-vivo* testing.

Conclusion

Docking analysis followed by lead optimization identified β-amyrin and lupeol as the most promising lead compounds for targeting all cobra venom toxic proteins. It was also noted that out of 14 cobra venom proteins screened, *C. gigantea* derived phytochemicals can inhibit all target proteins. In traditional medicine, this plant is not used alone but it is used as an ingredient of the compound herbal formulation and the *in-silico* screening results substantiate the traditional use of it as a part of a compound drug. However, *in-vitro* and *in-vivo* experiments are essential for confirmation.

Acknowledgments

We thank the Director, KSCSTE-Jawaharlal Nehru Tropical Botanic Garden and Research Institute, for providing facility and support. We gratefully thank the University of Kerala for the financial assistance.

References

1. Nisha NC, Sreekumar S, Biju CK. *In vitro and in-silico* validation of anti-cobra venom activity and identification of lead molecules in Aegle marmelos (L.) Correa. Current Sci. 2018 March 25;114(6):1214-21. doi: 10.18520/cs/v114/i06/1214-1221.
2. World Health Organization. Snakebite envenoming: a strategy for prevention and control, 2019. Available form: https://www.who.int/publications/i/item/9789241515641.
3. Nisha NC, Sreekumar S, Biju CK, Krishnan PN. Identification of lead compounds with cobra venom neutralizing activity in three Indian medicinal plants. Int J Pharm Pharm Sci. 2014 Jan;6:536-41.
4. Trott O, Olson AJ. AutoDock Vina: improving the speed and accuracy of docking with a new scoring function, efficient optimization, and multithreading. *J Comput Chem.* 2010 Jan 30;*31*(2):455-61. doi:10.1002/jcc.21334.
5. Shefin Basheera, Sreekumar S. Anti-Tuberculosis activity in *Punica granatum*: *In-silico* validation and identification of lead molecules. Indian J Pharm Sci. 2021 Jan;778. doi:10.36468/pharmaceutical-science.788.
6. Douglas EV Pires, Tom L Blundell, David BA. pkCSM: Predicting small-molecule pharmacokinetic and toxicity properties using graph-based signatures. J Med Chem. 2015 Apr 10;58(9):4066-72. doi: 10.1021/acs.jmedchem.5b00104.
7. Antoine Daina1, Olivier Michielin, VincentZoete. SwissADME: A free web tool to evaluate pharmacokinetics, drug-likeness, and medicinal chemistry friendliness of small molecules. Sci Rep. 2017 Mar 3;7:42717. doi:10.1038/srep42717.
8. Dennis EA, Cao J, Hsu YH, Magrioti V, Kokotos G. Phospholipase A_2 enzymes: Physical structure, biological function, disease implication, chemical inhibition, and therapeutic intervention. Chem Rev. 2011 Sept12;111(10):6130-85. doi: 10.1021/cr200085w.

9. Gutiérrez JM, Lomonte B. Phospholipases A_2: Unveiling the secrets of a functionally versatile group of snake venom toxins. Toxicon. 2013 Feb 1;62:27. doi: 10.1016/j.toxicon.2012.09.006.
10. Chang LS, Chou YC, Lin SR, Wu BN, Lin J, Hong E, Sun YJ, Hsiao CD. A novel neurotoxin, cobrotoxin B, from *Naja naja atra* (Taiwan cobra) venom: purification, characterization, and gene organization. J Biochem. 1997 Dec 1;122(6):1252-9. doi: 10.1093/oxfordjournals.jbchem.a021889.
11. Mohan SK, Yu C. Structure function relationships of cobrotoxin from *naja naja atra*. Toxin Rev. 2007 Jan 1;26(2):99-122. doi: 10.1080/15569540701209658.
12. Izidoro LF, Sobrinho JC, Mendes MM, Costa TR, Grabner AN, Rodrigues VM, da Silva SL, Zanchi FB, Zuliani JP, Fernandes CF, Calderon LA. Snake venom L-amino acid oxidases: Trends in pharmacology and biochemistry. Biomed Res Int. 2014 Mar 12;2014(1):196754. doi: 10.1155/2014/196754.
13. Paloschi MV, Pontes AS, Soares AM, Zuliani JP. An update on potential molecular mechanisms underlying the actions of snake venom L-amino acid oxidases (LAAOs). Curr Med Chem. 2018 Jun 1;25(21):2520-30. doi: 10.2174/0929867324666171109114125.
14. Du XY, Clemetson KJ. Snake venom L-amino acid oxidases. Toxicon. 2002 Jun 1;40(6):659-65. doi: 10.1016/S0041-0101(02)00102-2.
15. Tan KK, Bay BH, Gopalakrishnakone P. L-amino acid oxidase from snake venom and its anticancer potential. Toxicon. 2018 Mar 15;144:7-13. doi: 10.1016/j.toxicon.2018.01.015.
16. Vyas VK, Brahmbhatt K, Bhatt H, Parmar U. Therapeutic potential of snake venom in cancer therapy: current perspectives. Asian Pac J Trop Biomed. 2013 Feb 1;3(2):156-62. doi:10.1016/S2221-1691(13)60042-8.
17. Tougu V. Acetylcholinesterase: Mechanism of catalysis and inhibition. Cent Nerv Syst Agents Med Chem. 2001 Aug 1;1(2):155-70. doi: 10.2174/1568015013358536.
18. Taylor P, Radic Z. The cholinesterases: from genes to proteins. Annu Rev Pharmacol Toxicol. 1994 Apr;34(1):281-320. doi: 10.1146/annurev.pa.34.040194.001433.
19. Aroniadou-Anderjaska V, Figueiredo TH, de Araujo Furtado M, Pidoplichko VI, Braga MF. Mechanisms of organophosphate toxicity and the role of acetylcholinesterase inhibition. Toxics. 2023 Oct 18;11(10):866. doi: 10.3390/toxics11100866.
20. Akaike A, Takada-Takatori Y, Kume T, Izumi Y. Mechanisms of neuroprotective effects of nicotine and acetylcholinesterase inhibitors: role of α4 and α7 receptors in neuroprotection. J Mol Neurosci. 2010 Jan;40:211-6. doi: 10.1007/s12031-009-9236-1.
21. McGleenon BM, Dynan KB, Passmore AP. Acetylcholinesterase inhibitors in Alzheimer's disease. Br J Clin Pharmacol. 1999 Oct;48(4):471. doi: 10.1046/j.1365-2125.1999.00026.x.
22. Li Y, Hai S, Zhou Y, Dong BR. Cholinesterase inhibitors for rarer dementias associated with neurological conditions. Cochrane Database Syst Rev. 2015 Mar 3. doi: 10.1002/14651858.CD009444.pub3.
23. Walkinshaw MD, Saenger W, Maelicke A. Three-dimensional structure of the" long" neurotoxin from cobra venom. Proc Natl Acad Sci U S A. 1980 May;77(5):2400-4. doi: 10.1073/pnas.77.5.2400.
24. Ranawaka UK, Lalloo DG, de Silva HJ. Neurotoxicity in snakebite limits of our knowledge. PLoS Negl Trop Dis. 2013 Oct 10;7(10):2302. doi: 10.1371/journal.pntd.0002302.
25. Hiu JJ, Yap MK. The myth of cobra venom cytotoxin: More than just direct cytolytic actions. Toxicon: X. 2022 Jun 1; 14:100123. doi: 10.1016/j.toxcx.2022.100123.
26. Gasanov SE, Dagda RK, Rael ED. Snake venom cytotoxins, phospholipase A_2s, and Zn^{2+} -dependent metalloproteinases: mechanisms of action and pharmacological relevance. J Clin Toxicol. 2014 Jan 25;4(1):1000181. doi: 10.4172/2161-0495.1000181.
27. Neema KN, Hamse Kameshwar V, Nafeesa Z, Kumar D, Babu Shubha P, Nagendra Prasad MN, Swamy SN. Serine protease from Indian cobra venom: its anticoagulant property and effect on human fibrinogen. Toxin Rev. 2022 Jan 2;41(1):165-74. doi: 10.1080/15569543.2020.1855656.
28. Olaoba OT, Dos Santos PK, Selistre-de-Araujo HS, de Souza DH. Snake venom metalloproteinases (SVMPs): A structure-function update. Toxicon: X. 2020 Sep 1;7:100052. doi: 10.1016/j.toxcx.2020.100052.
29. Matsui T, Fujimura Y, Titani K. Snake venom proteases affecting hemostasis and thrombosis. Biochim Biophys Acta Protein Struct Mol Enzymol. 2000 Mar 7;1477(12);146-56. doi. 10.1016/S0167-4838(99)00268-X.
30. Sliwoski G, Kothiwale S, Meiler J, Lowe EW. Computational methods in drug discovery. Pharmacol Rev. 2014 Jan;66(1):334-95. doi: 10.1124/pr.112.007336.
31. Jorgensen WL. The many roles of computation in drug discovery. Sci. 2004 Mar 19;303(5665):1813-18. doi:10.1126/science.1096361.
32. Tan S, Li D, Zhu X. Cancer immunotherapy: Pros, cons and beyond. Biomed Pharmacother. 2020 Apr;81:8-10. doi: 10.1016/j.biopha.2020.109821.
33. Patani GA, LaVoie EJ. Bioisosterism: A rational approach in drug design. Chem Rev. 1996 Dec 19;96(8):3147-76. doi: 10.1021/CR950066Q.
34. Sarkar A, Concilio S, Sessa L, Marrafino F, Piotto S. Advancements and novel approaches in modified autodock vina algorithms for enhanced molecular docking. Results Chem. 2024 Jan 14:101319. doi:10.1016/j.rechem.2024.101319.
35. Rose PW, Bi C, Bluhm WF, Christie CH, Dimitropoulos D, Dutta S, Green RK, Goodsell DS, Prlić A, Quesada M, Quinn GB. The RCSB Protein Data Bank: New resources for research and education. Nucleic Acids Res. 2012 Nov 27;41(D1):D475-82. doi: 10.1093/nar/gks1200.
36. Sugathan KJ, Sreekumar S, Kamalan BC. *In-silico* screening and identification of lead molecules from *Garcinia gummi-gutta* with multitarget activity against SARS-CoV-2. J Appl Pharm Sci. 2024 July;14(7):124-32. doi: 10.7324/JAPS.2024.150413.
37. Morris GM, Huey R, Lindstrom W, Bevan DR, Dockett M, Sanner MF. AutoDock4 and AutoDockTools4: Automated docking with selective receptor flexibility. *J Comput Chem.* 2009 Apr 27;30(16):2785-91. doi: 10.1002/jcc.21256.
38. Balasubramanian K. Mathematical and computational techniques for drug discovery: promises and developments. Curr Med Chem. 2018 Dec 1;18(32):2774-99. doi: 10.2174/1568026619666190208164005.
39. Leelananda SP, Lindert S. Computational methods in drug discovery. Beilstein J Org Chem. 2016 Dec 12;12(1):2694-718. doi: 10.3762/bjoc.12.267.
40. Meyer E. Internal water molecules and H-bonding in biological macromolecules: A review of structural features with functional implications. Protein Sci. 1992 Dec;1(12):1543-62. doi: 10.1002/pro.5560011203.
41. Kollman PA, Massova I, Reyes C, Kuhn B, Huo S, Chong L, Lee M, Lee T, Duan Y, Wang W, Donini O, Cieplak P, Srinivasan J, Case DA, Cheatham TE. Calculating structures and free energies of complex molecules: combining molecular mechanics and continuum models. Acc Chem Res. 2000 Oct 4;33(12):889-97. doi: 10.1021/ar000033j.
42. Bera I, Payghan PV. Use of molecular dynamics simulations in structure-based drug discovery. Curr Pharm Des. 2019;25(31):3339-49. doi: 10.2174/1381612825666190903153043.
43. Fusani L, Palmer DS, Somers DO, Wall ID. Exploring ligand stability in protein crystal structures using binding pose metadynamics. J Chem Inf Model. 2020 Jan 7;60(3);1528-39. doi: 10.1021/acs.jcim.9b00843.
44. Fu Y, Zhao J, Chen Z. Insights into the molecular mechanisms of protein-ligand interactions by molecular docking and molecular dynamics simulation: A case of oligopeptide binding protein. Comput Math Methods Med. 2018 Dec 4;2018(1): 3502514. doi: 10.1155/2018/3502514.
45. Zhao H, Caflisch A. Molecular dynamics in drug design. Eur J Med Chem. 2015 Feb 16;91:4-14. doi: 10.1016/j.ejmech.2014.08.004.
46. Lin JH. Accommodating protein flexibility for structure-based drug design. Curr Top Med Chem. 2011;11(2):171-78. doi: 10.2174/156802611794863580
47. Du X, Li Y, Xia YL, Ai SM, Liang J, Sang P, Ji XL, Liu SQ. Insights into protein- ligand interactions: mechanisms, models, and methods.

Int J Mol Sci. 2016 Jan 26;17(2):144. doi: 10.3390/ijms17020144.
48. Fang Y. Ligand-receptor interaction platforms and their applications for drug discovery. Expert Opin. 2012 Oct;7(10):969-88. doi: 10.1517/17460441.2012.715631.
49. Melo CM, Morais TC, Tomé AR, Brito GA, Chaves MH, Rao VS, Santos FA. Anti-inflammatory effect of α, β-amyrin, a triterpene from Protium heptaphyllum, on cerulein-induced acute pancreatitis in mice. J Inflamm Res. 2011 Jul;60:673-81. doi: 10.1007/s00011-011-0321-x.
50. Liu K, Zhang X, Xie L, Deng M, Chen H, Song J, Long J, Li X, Luo J. Lupeol and its derivatives as anticancer and anti-inflammatory agents: Molecular mechanisms and therapeutic efficacy. Pharmacol Res. 2021 Feb;164:105373. doi: 10.1016/j.phrs.2020.105373.
51. Singh OP, Singh B Chakravarty J, Sundar S. Current challenges in treatment options for visceral leishmaniasis in India: A public health perspective. Infect Dis Poverty. 2016 Mar 8;5:19. doi: 10.1186/s40249-016-0112-2.

HOW TO CITE THIS ARTICLE: Aswathy C, Sreekumar S, Sugathan JK, Biju CK. *In-silico* Evaluation of Phytochemicals from *Calotropis gigantea* (L.) Dryand. for Multi-Target Inhibition of Cobra Venom Proteins. Int. J. Pharm. Sci. Drug Res. 2025;17(2):129-143. **DOI:** 10.25004/IJPSDR.2025.170203